Toxicology in Vitro 32 (2016) 166–180

Contents lists available at ScienceDirect

Toxicology in Vitro

journal homepage: www.elsevier.com/locate/toxinvit

Autophagic activity in BC3H1 cells exposed to yessotoxin

Mónica Suárez Korsnes [a,*], Hilde Kolstad [b], Charlotte Ramstad Kleiveland [a,e], Reinert Korsnes [c,d], Elin Ørmen [b]

[a] Department of Chemistry, Biotechnology and Food Science, Norwegian University of Life Sciences (NMBU) — Campus Ås, P.O. Box 5003, NO-1432 Ås, Norway
[b] Imaging Centre, Norwegian University of Life Sciences (NMBU) — Campus Ås, P.O. Box 5003, NO-1432 Ås, Norway
[c] Norwegian Institute of Bioeconomy Research (NIBIO), Ås, Norway
[d] Norwegian Defense Research Establishment (FFI), Kjeller, Norway
[e] Smerud Medical Research, Oslo, Norway

ARTICLE INFO

Article history:
Received 20 August 2015
Received in revised form 1 December 2015
Accepted 15 December 2015
Available online 30 December 2015

Keywords:
Autophagy
Yessotoxin
LC3-II
Atg proteins
Lamellar bodies
Autophagosomes
BC3H1 cells

ABSTRACT

The marine toxin yessotoxin (YTX) can induce programmed cell death through both caspase-dependent and -independent pathways in various cellular systems. It appears to stimulate different forms of cellular stress causing instability among cell death mechanisms and making them overlap and cross-talk. Autophagy is one of the key pathways that can be stimulated by multiple forms of cellular stress which may determine cell survival or death. The present work evaluates a plausible link between ribotoxic stress and autophagic activity in BC3H1 cells treated with YTX. Such treatment produces massive cytoplasmic compartments as well as double-membrane vesicles termed autophagosomes which are typically observed in cells undergoing autophagy. The observed autophagosomes contain a large amount of ribosomes associated with the endoplasmic reticulum (ER). Western blotting analysis of Atg proteins and detection of the autophagic markers LC3-II and SQSTM1/p62 by flow cytometry and immunofluorescence verified autophagic activity during YTX-treatment. The present work supports the idea that autophagic activity upon YTX exposure may represent a response to ribotoxic stress.

1. Introduction

Autophagy is a general term for cellular processes by which unnecessary or dysfunctional components including organelles are delivered to the lysosomes for degradation or for recycling (Levine and Kroemer, 2008; Mizushima et al., 2010). Normal autophagy is tightly regulated at a basal level to maintain cellular homeostasis whereas unregulated degradation of cytoplasmic contents can be lethal (Levine, 2005; Mizushima et al., 2008).

Autophagy has typically been considered in a context of cell survival (Levine and Kroemer, 2009). It may also play a role in programmed cell death. However, this role is hard to identify since autophagic activity in dying cells can be an attempt to survive (Tsujimoto and Shimizu, 2005; Kroemer et al., 2007).

The concept of autophagic cell death stems from observations of formation of autophagosomes and lysosomes in regions of cells where programmed cell death tend to take place (Tsujimoto and Shimizu, 2005). Autophagic cell death may also result from excessive levels of cellular self digestion (Levine, 2005).

It seems that some cytotoxic drugs can activate autophagic death in cells that are resistant to apoptosis such as those expressing BCl-2 anti-apoptotic proteins or those lacking Bax and Bak (Shimizu et al., 2004; Yu et al., 2004). Such cells can contain various autophagosomes, but their presence can be abolished by treatment of autophagy inhibitors or by silencing Atg5 and Atg6 proteins (Tsujimoto and Shimizu, 2005).

The role of autophagy as a programmed cell death mechanism is unclear. However, it can provide nutrients to the cells to survive or recycle components necessary for organ morphogenesis and tissue remodelling. The autophagic process might in this case have an advantage over apoptotic cell death reducing the workload of phagocytes (Tsujimoto and Shimizu, 2005; Kroemer et al., 2007). Elimination of cancer cells by activation of autophagic activity has been reported (Liang et al., 1999; Yue et al., 2003; Qu et al., 2003). Autophagy plays a role in cellular immune responses, especially when it precedes cell death (Ma et al., 2013). It can take part within ciliogenesis and control of cilia length to sense various extracellular changes (Orhon et al., 2014).

Mammalian autophagy involves many molecular components (Kroemer et al., 2010). Two of these components are ubiquitin-like proteins called Atg12 and Atg8/LC3 conjugation systems. They are essential for formation and maturation of autophagosomes and signalling to regulate autophagy (Yang and Klionsky, 2010a). The core pathway of mammalian autophagy begins with the formation of the isolation membrane (phagophore) which can be in close proximity to subcellular structures like mitochondria and endoplasmic reticulum (ER), where MAMS (mitochondria-associated ER membranes) facilitates the recruitment of the Atg5–Atg12–Atg16 complex indispensable for the autophagosome

* Corresponding author.
E-mail address: monica.suarez.korsnes@nmbu.no (M.S. Korsnes).

http://dx.doi.org/10.1016/j.tiv.2015.12.010

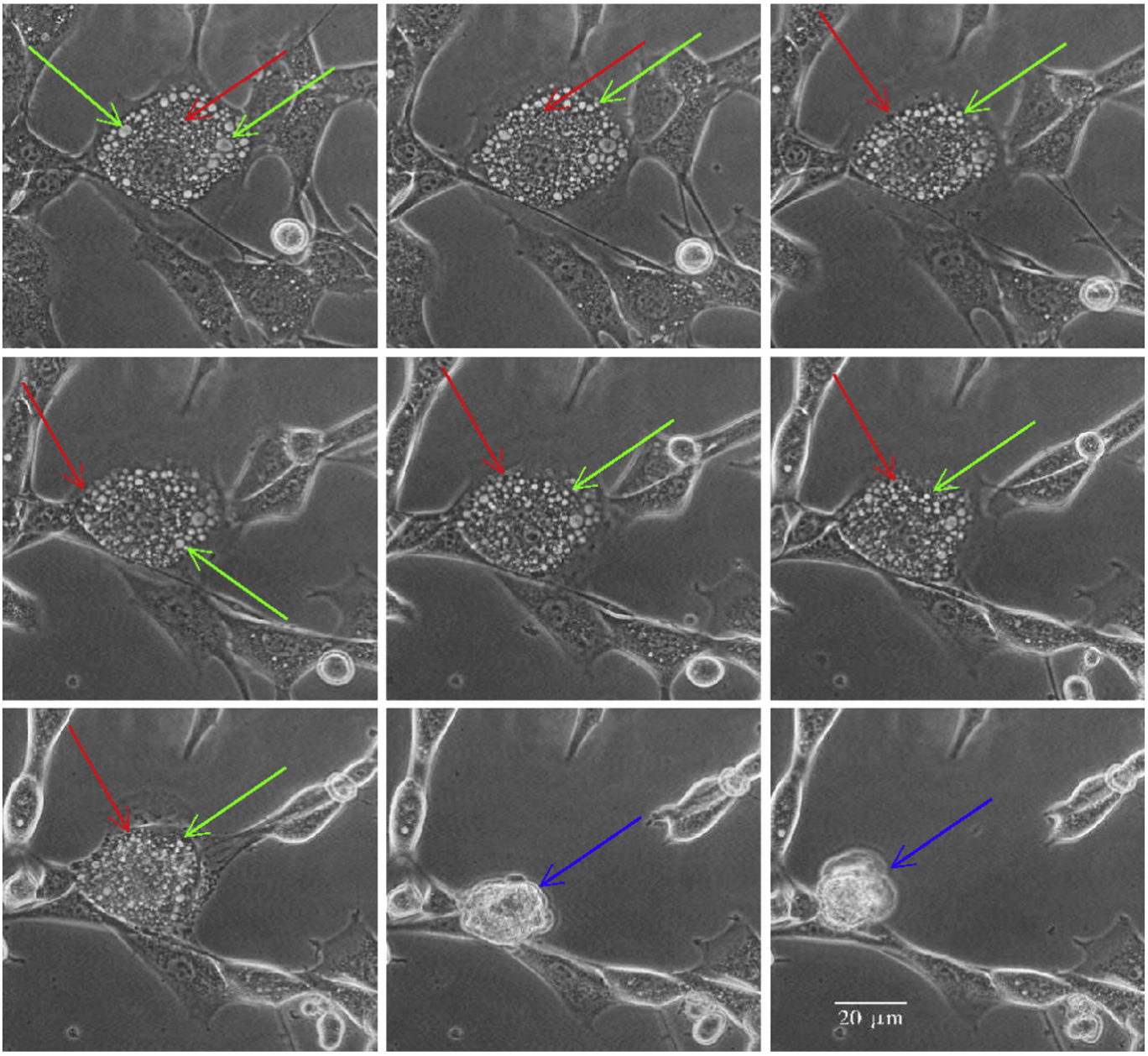

Fig. 1. Subsequent phase contrast images, 25 min apart, showing cytoplasmic vacuolisation in BC3H1 cells upon 100 nM YTX treatment. Green arrows indicate membrane-enclosed vacuoles, and red arrows indicate membranous dense bodies. Blue arrow marks sign of cell death.

formation (Ma et al., 2013). The proximity of the phagophore to the MAMS may facilitate a connection between autophagy and activation of stress response pathways (Hamasaki et al., 2013).

The marine toxin yessotoxin (YTX) is a polyether compound produced by the dinoflagellates *Protoceratium reticulatum* and *Gonyaulax grindleyi* (Satake et al., 1997; Satake et al., 1999; Draisci et al., 1999). The toxin was initially isolated from the digestive gland of scallops *Pactinopecten yessoensis* (Murata et al., 1987). It can trigger a broad spectrum of cellular effects of possible medical interest (Korsnes et al., 2006; López et al., 2008; L.M.B. López et al., 2011; Korsnes, 2012; A.M. López et al., 2011; Alonso et al., 2013; Korsnes et al., 2014). YTX mechanisms of action vary among cells and they appear to be cell-specific and concentration-dependent (De la Rosa et al., 2001; Alfonso et al., 2003; Franchini et al., 2004; Malagoli et al., 2006; Callegari and Rossini, 2008; Ronzitti and Rossini, 2008; Young et al., 2009; Orsi et al., 2010; Martn-López et al., 2012; Fernández-Araujo et al., 2015).

YTX can trigger diverse signalling pathways involving stress responses such as endoplasmic reticulum and ribotoxic stress (Rubiolo et al., 2014; Korsnes et al., 2014). Autophagy is one of the key pathways mediating diverse stress responses (Kroemer et al., 2010). Cellular stress response may determine whether cells can adapt their metabolism and protect themselves against damage. Autophagy constitutes therefore a protective mechanism in response to stress and eliminate damaged components through metabolism and recycling to maintain nutrient and cellular homeostasis (Kroemer et al., 2010). Autophagy may also target specific organelles such as ER, mitochondria, peroxisomes and ribosomes. Such types of autophagy are respectively referred to as reticulophagy, mitophagy, pexophagy and ribophagy (Ma et al.,

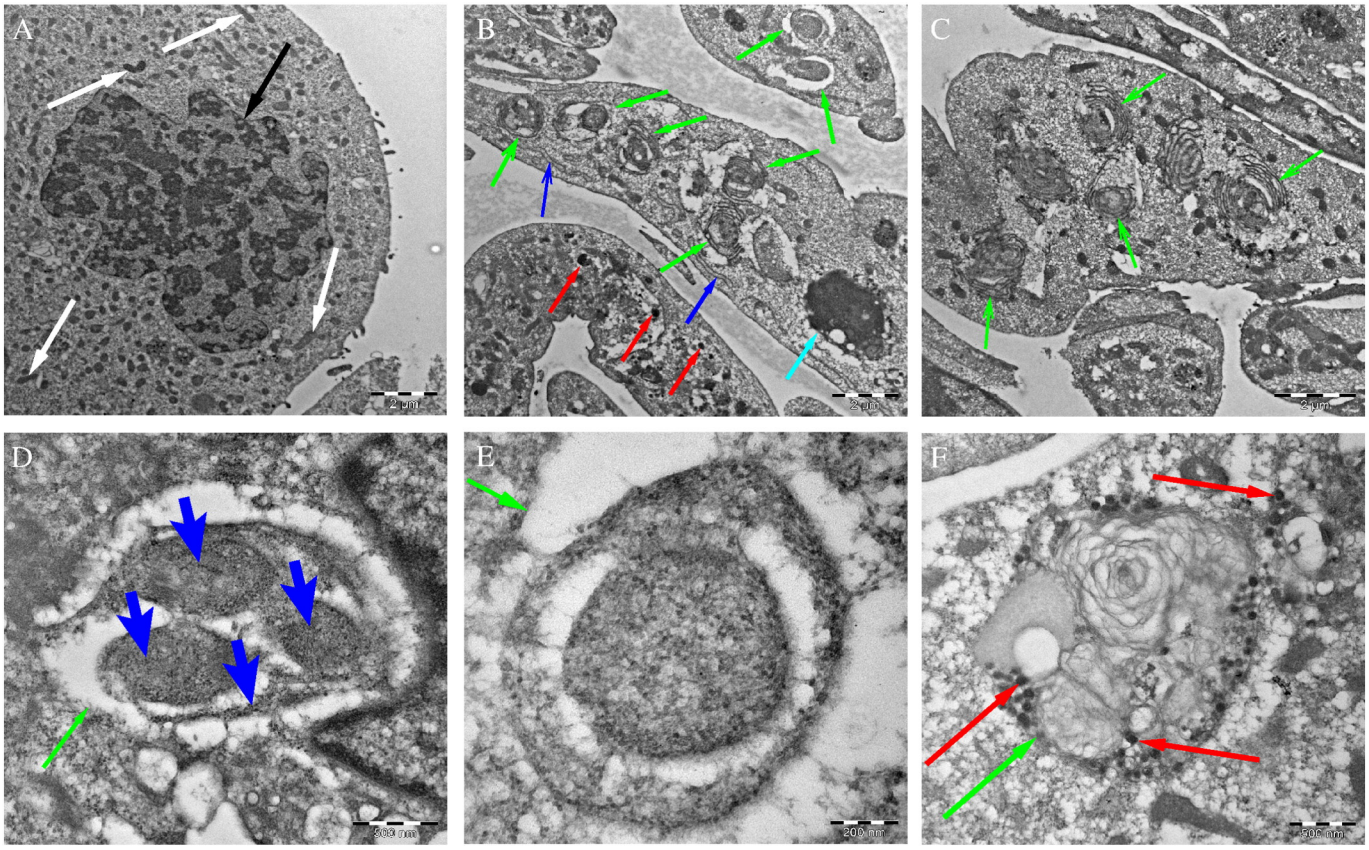

Fig. 2. Transmission electron microscopy images showing autophagic compartments in BC3H1 cells exposed to 100 nM YTX for 24 h. A) Control cell displaying normal morphology. Black arrow points on nucleus and white arrows show mitochondria. B) Treated cell where green arrows point on autophagosomes. Light blue arrow shows an autolysosome; dark blue arrows show endoplasmic reticulum (ER) and red arrows show lipid droplets. C) Green arrows show lamellar bodies in a treated cell. D) Detailed view showing endoplasmic reticulum and ribosomes (blue arrows) inside the autophagosome (green arrow). E) Detailed view of autophagosome showing ribosomes associated with the ER (green arrow). F) Detailed view of a lamellar body (green arrow). Note the presence of lipid droplets (red arrows).

2013). However, the relation between ribotoxic stress and autophagy have not been clarified under YTX exposure.

The present work evaluates if the generation of ribotoxic stress in BC3H1 cells upon YTX exposure can activate autophagic activity. This model system has revealed induction of different cell death pathways, 28SrRNA cleavage and protein synthesis inhibition under YTX-treatment (Korsnes, 2012; Korsnes et al., 2014). YTX also induces phosphorylation of the double-stranded RNA-associated protein kinase (PKR) and MAPK signalling activation (Korsnes et al., 2014). PKR and MAPK have previously been shown to promote autophagy (Tallóczy et al., 2006; Pattingre et al., 2009).

YTX interaction with the ribosome might cross-talk with ER stress response. A defective translation by damaged ribosomes might cause accumulation of misfolded heat shock proteins (Hsp70) which are located in the lumen of the ER. Excess of Hsp70 containing complexes could enter the autophagic pathway for degradation and Korsnes et al. (2013) previously showed activation of Hsp70 in BC3H1 cells treated with 1-desulfoyessotoxin, a YTX analogue with a slight modification in its chemical structure.

Observation of ribosomes associated with the ER inside autophagosomes in YTX exposed cells suggests activation of selective autophagy called ribophagy. Such selective degradation of ribosomes may be considered as an attempt to preserve cellular homeostasis avoiding translation of potentially harmful or misfolded proteins that might accumulate during ribotoxic stress. Activation of autophagic activity by ribotoxic stress can therefore also be an additional quality control by specifically eliminating non-functional, incorrectly assembled, and/or damaged ribosomes to preserve cellular homeostasis.

2. Materials and methods

2.1. Toxin

YTX was provided by Christopher O. Miles at the National Veterinary Institute of Norway. YTX was dissolved in methanol as a 50 μM stock solution. The stock solution was diluted in Dulbecco's modified Eagle's medium (DMEM, Sigma), achieving a final concentration of 100 nM YTX in 0.2% methanol. Treated cells were incubated with 100 nM YTX and control cells were incubated with 0.2% methanol as vehicle. Control cells and treated cells were exposed to different end points (24 h, 48 h and 72 h).

2.2. Cell culture

BC3H1 cell lines were isolated from primary cultures derived from mouse (ATCC Number CRL-1443). Recent data suggest that BC3H1 cells closely resemble cells in an arrested state of skeletal muscle differentiation than smooth muscle cells. BC3H1 cells are easy to grow as monolayer and they have shown responsiveness, long cell life span and stability during YTX treatment. They were purchased from the American Type Culture Collection (Manassas, USA). BC3H1 cells were cultured in Dulbecco's modified Eagle's medium (DMEM, Lonza, Norway) supplemented with 20% foetal calf serum (FCS, Bionordika,

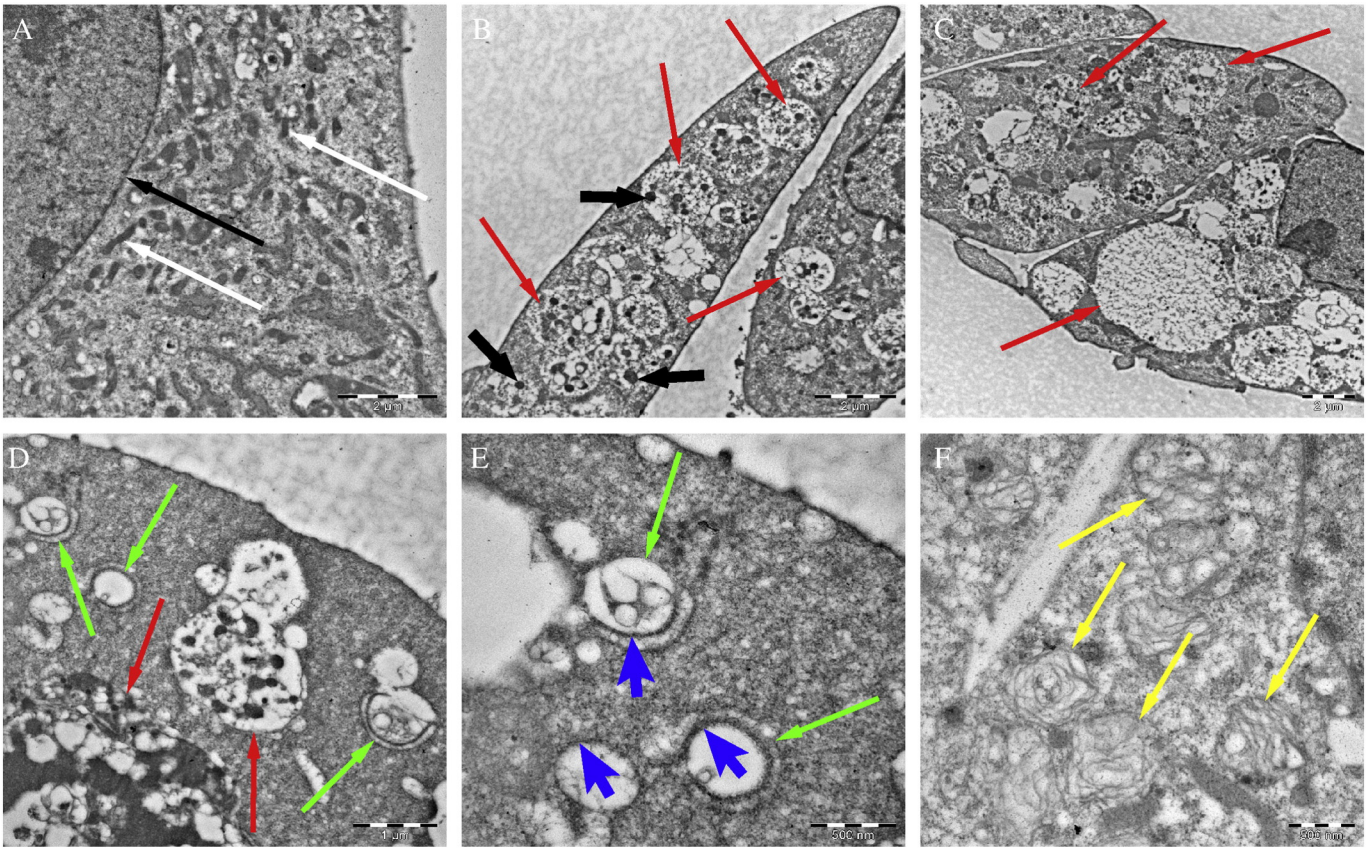

Fig. 3. Transmission electron microscopy images showing autophagic compartments in BC3H1 cells exposed to 100 nM YTX for 48 h. A) Control cell displaying normal morphology. Black arrow points on nucleus and white arrows show mitochondria. B) Treated cell where red arrows point on autolysosomes. Note the presence of lipid droplets (thick black arrows). C) Treated cell containing autolysosomes with partially degraded contents (red arrows). D) Detailed view of autophagosomes (green arrows) and autolysosomes (red arrows). E) Detailed view of autophagosomes (green arrows). Note ribosomes inside the autophagosome (blue arrows). F) Detailed view of several lamellar bodies (yellow arrows).

Norway). Cells were grown in a T75 culture vessel in 10 ml DMEM. Low passage numbers were used to perform experiments. Cells were maintained undifferentiated at 37 °C in a humidified 5% CO_2 atmosphere.

2.3. Transmission electron microscopy

BC3H1 cells were harvested and fixed with 2.0% paraformaldehyde and 1.25% glutaraldehyde in sodium cacodylate buffer (0.1 M, pH 7.2) for 3 h at room temperature. After fixation the cells were washed with cacodylate buffer postfixed with 1% osmium tetroxide in cacodylate buffer for 1.5 h at room temperature. BC3H1 cells were washed with cacodylate buffer, and embedded in 3% low melting agarose. Subsequently, the cells were washed thoroughly in cacodylate buffer and dehydrated with a graded ethanol series (50%, 70%, 90%, 96% and 4X 100%), 12 min for each step. The cells were then embedded in LR White resin (London Resin Company EMS, England).

Ultrathin sections were obtained with an ultramicrotome (LEICA EM UC 6) and sections were picked up with formvar- and carbon-coated slot copper grids. Counterstaining was performed with 4% aqueous uranyl acetate and 1% $KMNO_4$ for 10 min. The sections were examined with a FEI Morgani 268 transmission electron microscope at an accelerating voltage of 80 kV, and micrographs were recorded on a Veleta camera.

2.4. Immunofluorescence

3×10^5 control and YTX treated cells were fixed in 4.0% paraformaldehyde pH 7.3 for 15 min. In brief, after fixation, cells were washed 3 times with PBS and incubated in blocking solution 5% donkey serum diluted in 1% in PBS and 0.3% Triton X-100 for 1 h. Cells were stained with the anti-LC3-II antibody (1:200, Cell Signalling, USA) overnight at 4 °C. Cells were washed 3 times with PBS. Cells were then incubated 1 h with fluorescein (FITC)-conjugated donkey anti-rabbit (1:500, Jackson Immuno Research, USA), Hoechst 33342 (0.1 μg/ml, Molecular Probes, USA). Cells were examined with a Leica confocal laser scanner microscope SP5 (Leica Microsystems Wetzlar GmbH, Wetzlar, Germany).

2.5. Lysosomal assessment using LysoTracker Red DND-99 staining

1×10^4 control and YTX treated cells were fixed in 4.0% paraformaldehyde pH 7.3 for 30 min at room temperature. After fixation, cells were washed 3 times with PBS. The fixative was then replaced with prewarmed Live cell imaging solution containing 50 nM LysoTracker Red DND-99 (Life Technologies), and the cells were further incubated for 30 min at 37 °C. Cells were analysed with a Leica confocal laser scanner microscope SP5 (Leica Microsystems Wetzlar GmbH, Wetzlar, Germany).

2.6. Flow-cytometry

2×10^6 control and YTX treated cells were harvested and collected by centrifugation. In brief, cells were resuspended in 1 ml 1X PBS pH 7.2 and fixed in 4.0% paraformaldehyde for 10 min at 37 °C. Cells were chilled on ice for 1 min. The fixative was removed prior to permeabilisation by centrifugation and the cells were permeabilised

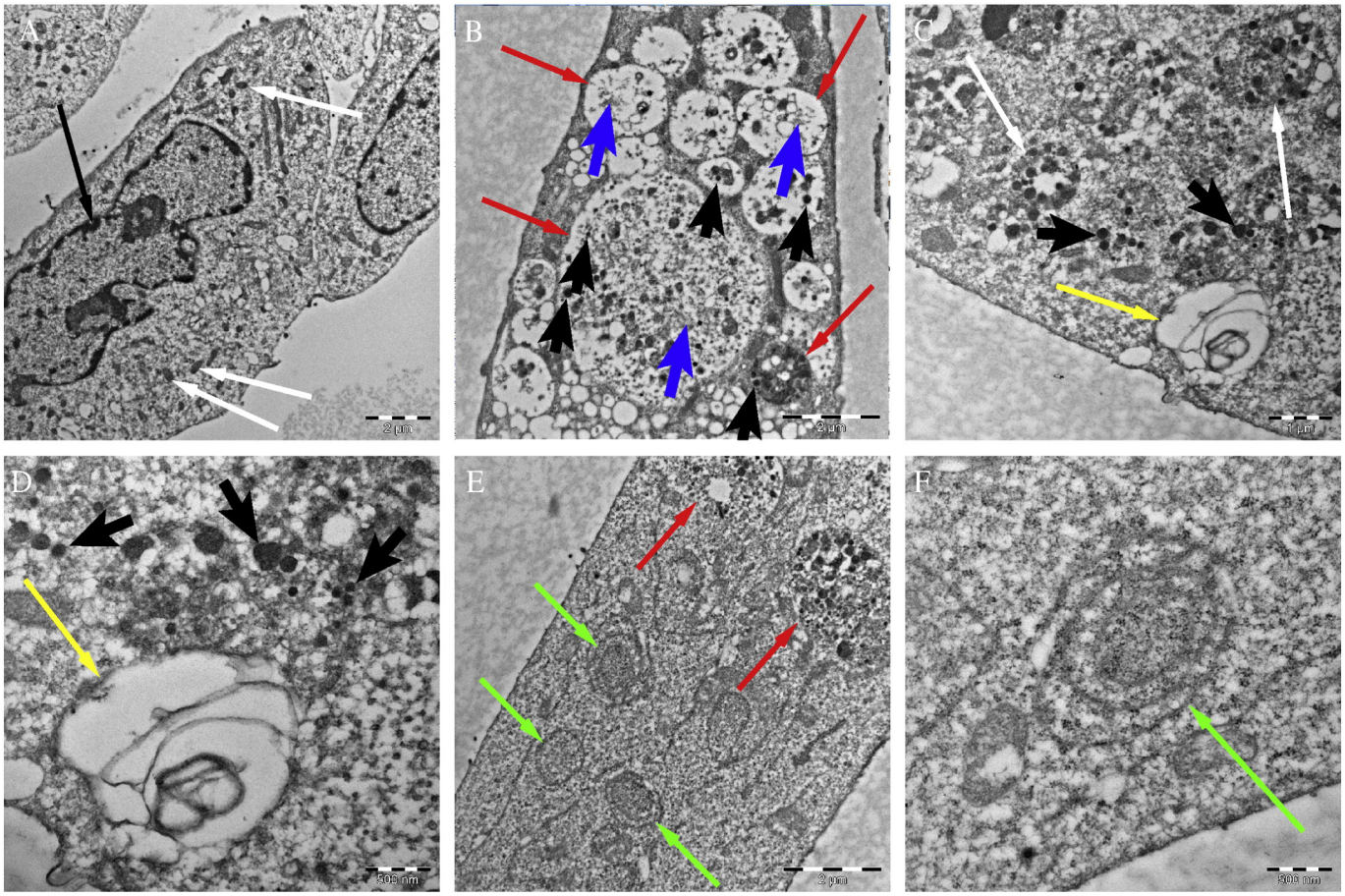

Fig. 4. Transmission electron microscopy images showing autophagic compartments in BC3H1 cells exposed to 100 nM YTX for 72 h. A) Control cell displaying normal morphology. Black arrow points on nucleus and white arrows show mitochondria. B) Treated cell containing autolysosomes (red arrows). Blue arrows show ribosomes and black arrows show lipid droplets. C) Autolysosomes (white arrows) in a treated cell. Yellow arrow shows a lamellar body. Note lipid droplets inside autolysosome (black thick arrows). D) Detailed view of a lamellar body (yellow arrow) and lipid droplets (black arrows). E) Detailed view of ribosomes associated with endoplasmic reticulum (green arrows) and autolysosomes (red arrows). F) Close view of ribosomes associated with endoplasmic reticulum (green arrow).

by adding ice-cold 90% methanol. Cells were incubated for 30 min on ice. 1×10^5 cells were resuspended in 500 μl incubation buffer (0.5% BSA in 1X PBS) and rinsed two times by centrifugation. Cells were blocked in incubation buffer for 10 min at room temperature and incubated in LC3II or p62 antibody (prepared in incubation buffer at 1:400 dilution) for 1 h at room temperature. Cell were then washed by centrifugation in 2 ml incubation buffer. Cells were incubated in fluorochrome-conjugated secondary antibody fluorescein (FITC)-conjugated donkey anti-rabbit (1:1000, Jackson Immuno Research, USA) diluted in incubation buffer for 30 min at room temperature. Cells were washed by centrifugation in 2 ml incubation buffer and finally resuspended in 0.5 ml PBS and analysed using a MACSQuant analyzer (Miltenyi Biotec GmBH, Bergisch Gladbach, Germany), following the manufacturer's instructions. The fluorescence of the FITC probe was analysed using 495 nm excitation and 519 emission wavelengths. Statistical analysis were performed using LibreOffice Calc providing computation of confidence intervals.

2.7. Western blotting analysis

Western blot analysis was performed by using the anti-Beclin, anti-Atg16, anti-LC3I/II and anti-p62 antibodies (cell signalling). Briefly, control and YTX-treated cells were trypsinised and centrifuged at 600 ×*g* for 10 min at 4 °C. 2×10^6 cells were resuspended in 100 μl lysis extraction buffer containing 25 mM Tris, pH 7.5, 100 mM NaCl, 20 mM NaF, 1 mM orthovanadate, 1% NP-40 and protease inhibitors.

Lysates were placed for 30 min on ice and centrifuged at 13,000 rpm for 10 min. The supernatants were transferred to an Eppendorf tube and collected as cytosolic fractions. 120 μg of protein was separated on a 12% Bis-Tris polyacrylamide gels (BioRad) for 1 h at 200 V, transferred onto a PVDF membrane and blocked with 5% nonfat dry milk in PBS. The membrane was probed with anti-Beclin, anti-Atg16, anti-LC3I/II and anti-p62 antibodies diluted 1:1000, overnight at 4 °C The membranes were washed with PBST (3 × 15 min) and incubated with a secondary antibody (goat anti-rabbit) labelled with alkaline phosphatase, diluted 1:4000. Immunoblotted bands were visualised by using a Visualizer Luminata Crescendo Western HRP substrate (Millipore) and the membranes were exposed to X-ray film for at least 2 min (Pierce, Il, USA). Western blot bands were scanned from film and quantitively analysed using the public domain computer program ImageJ. LibreOffice Calc was used to compute confidence intervals.

3. Results

YTX can induce autophagic activity in BC3H1 cells. This assessment results from experiments on such cells exposing them with 100 nM YTX for 24, 48 and 72 h and using phase contrast imaging, electron microscopy, Western blotting, flow cytometry and immunofluorescesce.

Phase contrast microscopy showed massive vacuolisation upon YTX-treatment. Massive vacuolisation in some experimental settings is typically observed in cells undergoing autophagy (Fig. 1).

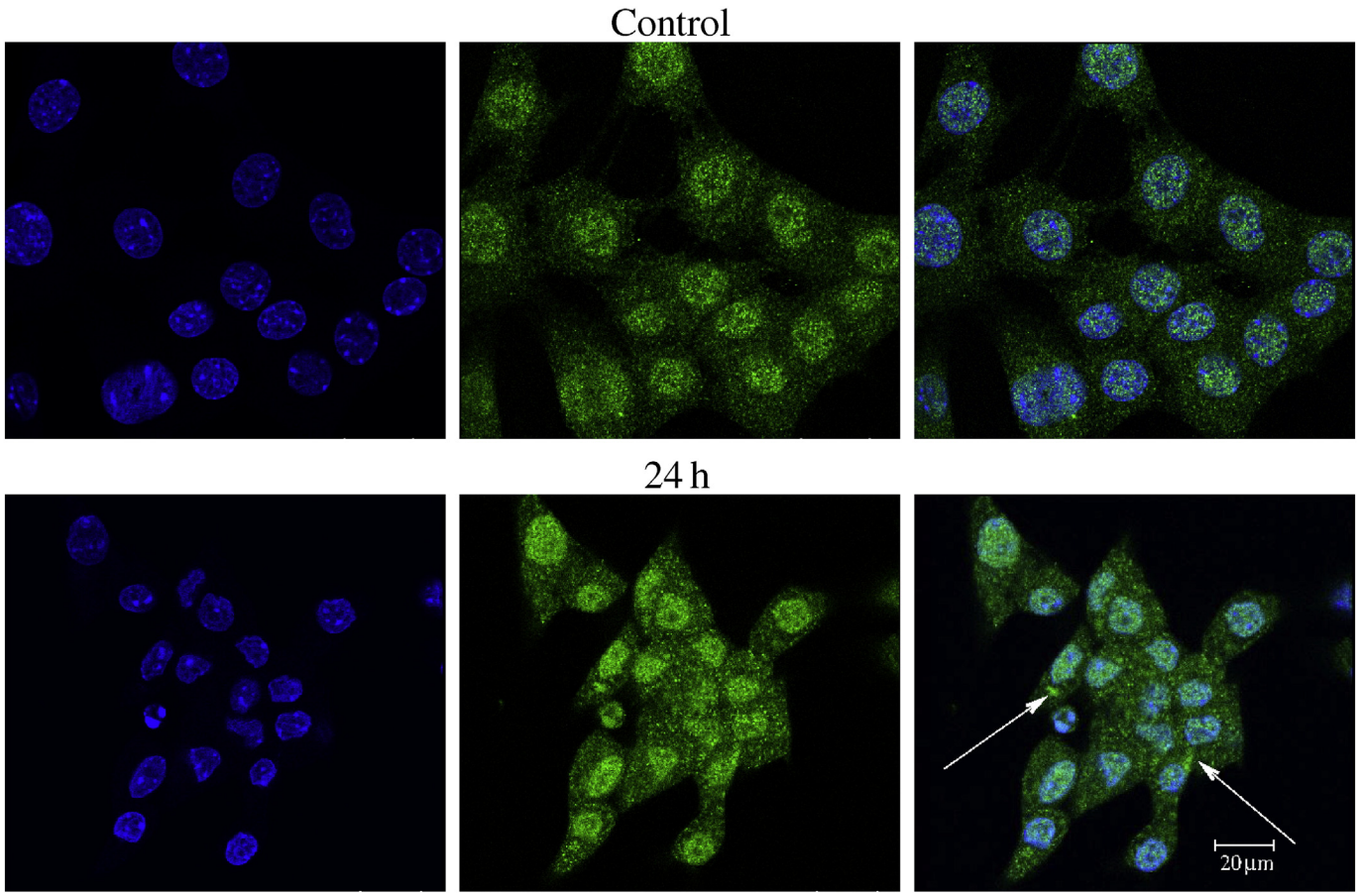

Fig. 5. Immunofluorescence detection of cytoplasmatic LC3-II puncta in BC3H1 cells exposed to 100 nM YTX for 24 h. Upper row: Control BC3H1 cells. Left: Hoechst labelling showing nuclei. Middle: Untreated BC3H1 cells. Right: Two-colour overlay with Hoechst and FITC showing diffuse cytoplasmic puncta. Lower row: YTX-treated cells. Left: Hoechst labelling showing nuclei. Middle: BC3H1 cells exposed for 24 h with 100 nM YTX. Right: Immunofluorescence staining of endogeneous LC3-II visualised as a cytoplasmatic puncta representing autophagosomes. Arrows at right in lower row show punctuate pattern indicating formation of autophagosomes. The results are representative for more than three independent experiments.

Transmission electron microscopy (TEM) evidenced the presence of various autophagic compartments such as autophagosomes, autolysosomes and lamellar bodies (Figs. 2, 3 and 4). Lamellar bodies have been observed in cells with defective lipid transport and autophagic activity (Schmitz and Müller, 1991). Double membrane structures with cytoplasmatic contents indicate autophagosmes. They may contain cytoplasmatic content with different fragments of organelles such as endoplasmic reticulum, mitochondria, ribosomes and other organellar fragments. Lamellar bodies and lipid droplets were also displayed in YTX-treated cells.

The punctuate distribution of autophagosomes was assessed by immunofluorescence detection of the mammalian autophagy protein LC3-II. LC3 is after synthesis processed at its C terminus by Atg4 and becomes LC3-I. LC3-I is subsequently conjugated with phosphatidylethanolamine (PE) to become LC3-II. LC3-II associates with both the inner and the outer membranes of the autophagosome and therefore it has become a good marker for autophagy (Mizushima et al., 2008; Klionsky et al., 2012). LC3-II puncta was visualised by fluorescence microscopy as a diffuse cytoplasmatic pool in untreated cells and as punctate structures representing autophagosomes in YTX-treated cells (Figs. 5, 6 and 7).

Serum starvation is often used experimentally to induce autophagy. Cells treated with lysotropic agents such as bafilomycin A1, which inhibit the autophagosome–lysosome function, can block degradation of LC3-II resulting in the accumulation of autophagosomes. Immunofluorescence detection of cytoplasmatic LC3-II puncta in treated and untreated BC3H1 cells subjected to starvation for 18 h, evidenced autophagosome accumulation. Starved cells exposed to YTX and bafilomycin treatment also evidenced increased LC3-II cytoplasmatic puncta, suggesting increased formation of autophagosomes due to the ability of both compounds to block the fusion with lysosomes (Fig. 8).

Flow-cytometry showed a temporal increase in expression levels of LC3-II in YTX-treated cells (Fig. 9). Treatment with 10 nM bafilomycin A1 slightly increased the level of the fluorescence signal after 24 h of YTX-treatment. Bafilomycin may therefore prevent maturation of autophagic vacuoles during this time. No significant change in the fluorescence signal was observed after 48 and 72 h YTX-treatment suggesting that bafilomycin treatment may not inhibit autophagosome formation.

Flow-cytometry analysis of SQSTM1/p62 evidenced a decrease in the fluorescence signal as compared to control (Fig. 10), suggesting autophagic activity in YTX-treated cells.

Western blotting analysis was performed with some of the proteins associated with the autophagic pathway such as Atg16, Beclin, LC3I/II and SQSTM1/p62. The Atg16 protein level increases with time (Fig. 11). This protein has been used to monitor movements of the plasma membrane as a donor of autophagy, and at an early stage of the autophagic process it locates in the phagophore, but not on completed autophagosomes (Ravikumar et al., 2010).

Fig. 12 shows that levels of Beclin-1 increase with time. This might indicate autophagic cell death, since Beclin levels remain low during survival and increase during autophagic cell death. Beclin also takes part in formation of autophagosomes (Tsujimoto and Shimizu, 2005).

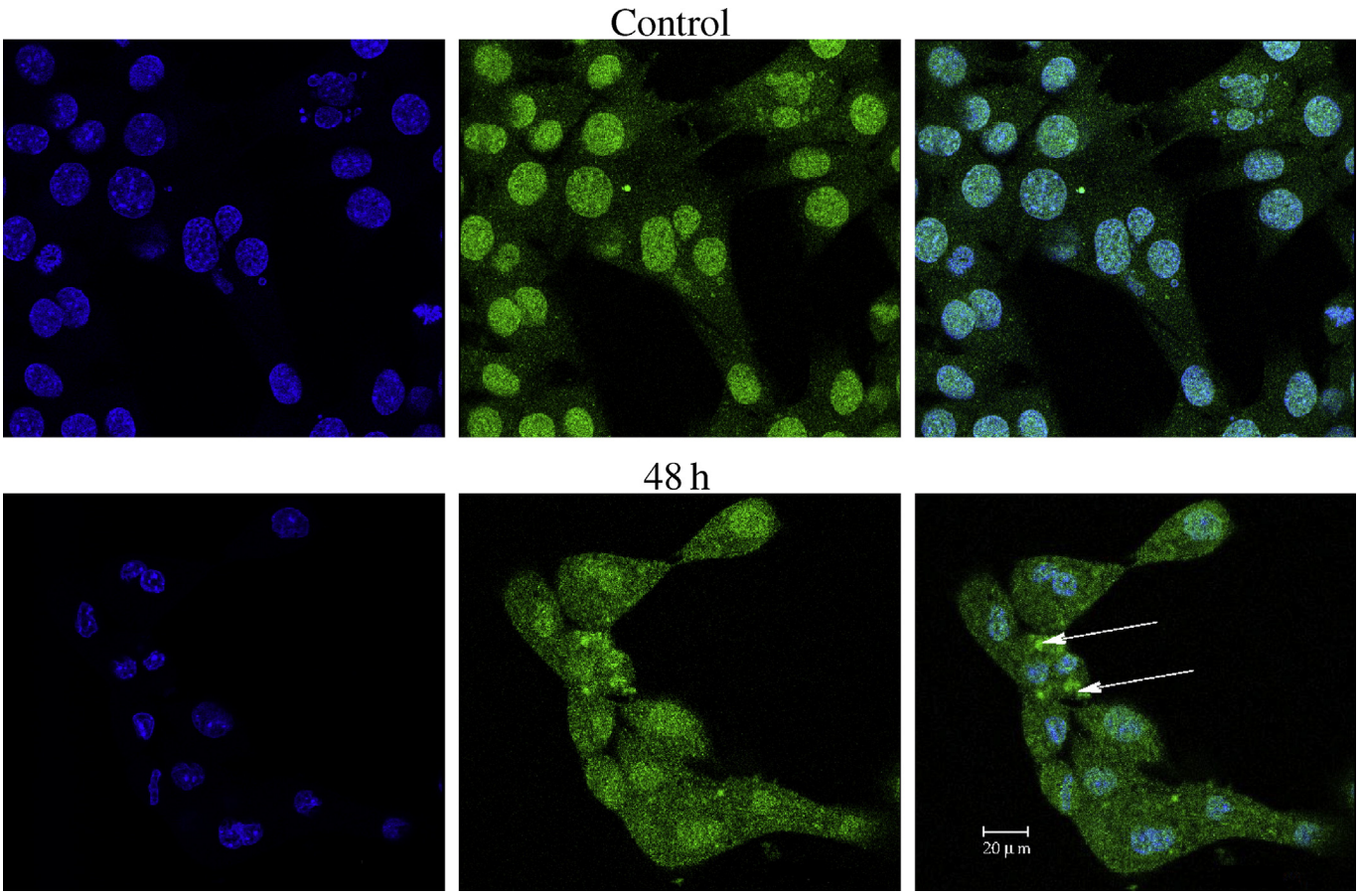

Fig. 6. Immunofluorescence detection of cytoplasmatic LC3-II puncta in BC3H1 cells exposed to 100 nM YTX for 48 h. Upper row: Control BC3H1 cells. Left: Hoechst labelling showing nuclei. Middle: Untreated BC3H1 cells. Right: Two-colour overlay with Hoechst and FITC showing diffuse cytoplasmic puncta. Lower row: YTX-treated cells. Left: Hoechst labelling showing nuclei. Middle: BC3H1 cells exposed for 48 h with 100 nM YTX. Right: Immunofluorescence staining of endogeneous LC3-II visualised as a cytoplasmatic puncta representing autophagosomes. Arrows at right in lower row show punctuate pattern indicating the formation of autophagosomes. Note more puncta in 48 h exposure as compared to 24 h. The results are representative for more than three independent experiments.

The ratio of LC3-II to LC3-I appears to correlate with changes in autophagy and it provides a more accurate measure of autophagic flux than ratios based on the total levels of LC3-II (Klionsky et al., 2012). LC3 turnover assay to monitor autophagic flux was measured by Western blotting using the ratio between LC3-I and LC3-II (Fig. 13). YTX increased the protein levels of LC3-II appearing to be maximal at 48 h. The apparent decrease of LC3-II levels at 72 h might be due to lysosomal degradation. This result conforms with the increased number of lysosomes observed at 72 h YTX exposure by transmission electron microscopy (Fig. 4).

Decrease in level of SQSTM1/p62 is associated with autophagy activation. Measurements of SQSTM1/p62 can also be used to monitor autophagic flux. P62 is selectively incorporated into autophagosomes where it binds directly to LC3-II and it degrades in the autolysosome. Fig. 14 evidences a notable decrease in the level of this protein showing a most prominent downregulation at 24 h YTX exposure.

Labelling of acidic vacuoles was performed with the fluorescent dye LysoTracker Red which accumulates in vesicles with an acidic pH. These acidic compartments, visualised as red puncta increased in treated cells over time (Fig. 15).

4. Discussion

The marine toxin YTX can induce different signalling pathways for programmed cell death (Korsnes et al., 2011; Korsnes, 2012; Rubiolo et al., 2014; Fernández-Araujo et al., 2015). The present experiments on BC3H1 cells evidences an accompanying active autophagic flux during this presumably regulated death process. The work adds observations to the debate on whether change in autophagic flux can be considered as part of the machinery of programmed cell death and hence in this way potentially play an evolutionary conserved role in organism-scale regulation.

YTX causes BC3H1 cells to develop an increased number of autophagic compartments such as vacuoles, autophagosomes, autolysosomes and lamellar bodies. Determination of early and late autophagic structures provides ultrastructural information on the autophagic process (Klionsky et al., 2012). Early autophagic vacuoles typically contain morphologically intact cytoplasm such as ribosomes and endoplasmic reticulum. Their limiting membranes are moderately visible via electron microscopy (Fig. 2). Late autophagic structures contain partially degraded organelles and the limiting membrane is not clearly visible from such imagery (Figs. 3 and 4). Correct identification of autophagic structures and proper analysis of their relation to other membrane-bound bodies in cells are necessary for correct interpretation of the dynamics during the autophagic process (Eskelinen, 2008; Eskelinen et al., 2011; Biazik et al., 2015).

Autophagy might target specific organelles or intracellular entities of the cytoplasm that are marked for destruction by ubiquitination. Such selective autophagy are referred to as “mitophagy”, “reticulophagy” or “ribophagy” for respective destruction of mitochondria, endoplasmic reticulum and ribosome (Ma et al., 2013). Figs. 2 (D and E) and 3 (D and E) show autophagosomes containing ribosomes associated with

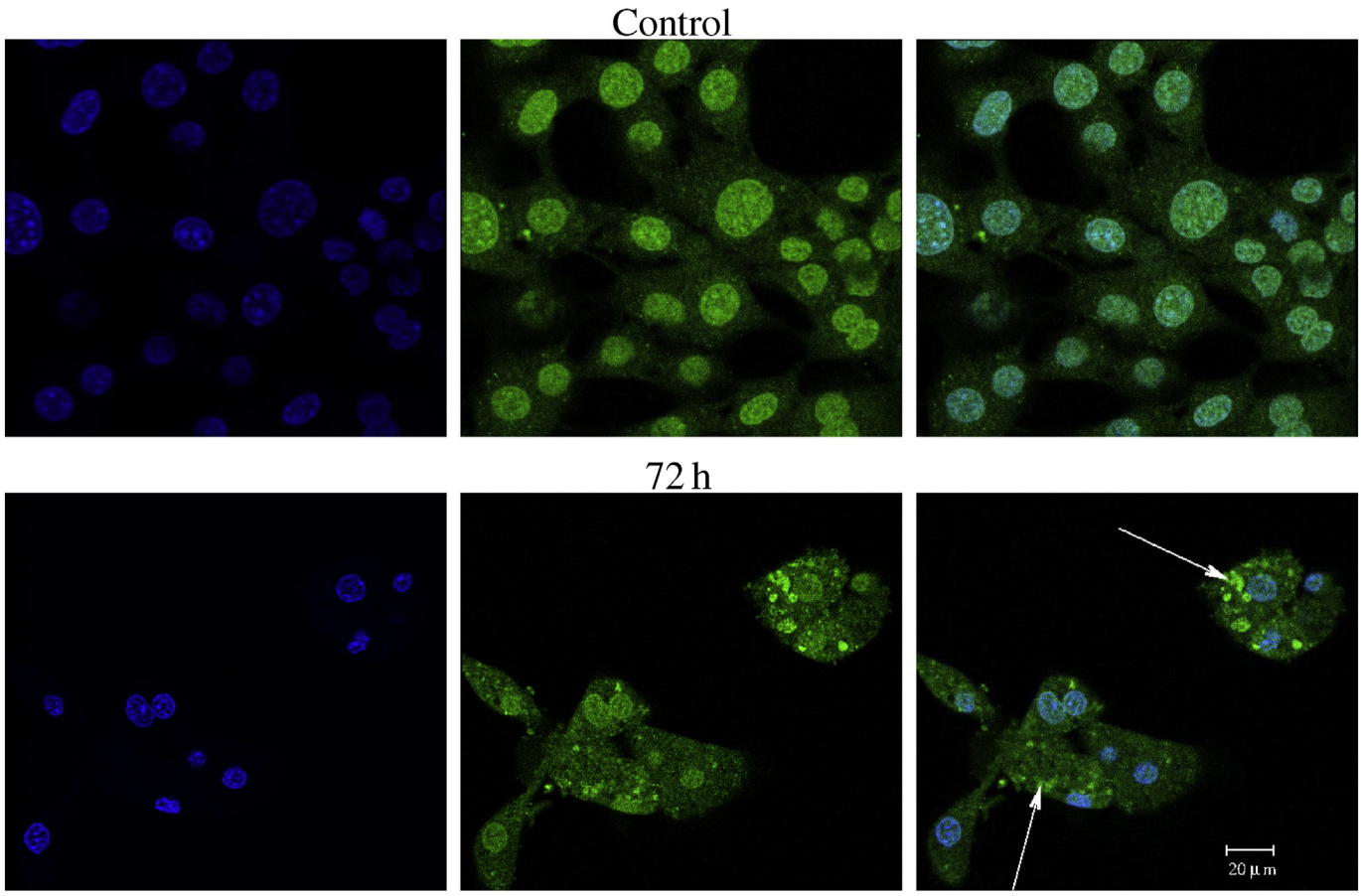

Fig. 7. Immunofluorescence detection of cytoplasmatic LC3-II puncta in BC3H1 cells exposed to 100 nM YTX for 72 h. Upper row: Control BC3H1 cells. Left: Hoechst labelling showing nuclei. Middle: Untreated BC3H1 cells. Right: Two-colour overlay with Hoechst and FITC showing diffuse cytoplasmic puncta. Lower row: YTX-treated cells. Left: Hoechst labelling showing nuclei. Middle: BC3H1 cells exposed for 72 h with 100 nM YTX. Right: Immunofluorescence staining of endogeneous LC3-II visualised as a cytoplasmatic puncta representing autophagosomes. Arrows at right in lower row show punctuate pattern indicating the formation of autophagosomes. Puncta also increases at 72 h exposure. The results are representative for more than three independent experiments.

endoplasmic reticulum. This may indicate selective destruction of ribosomes. This indication conforms to the observation that YTX treatment can cause rRNA cleavage and inhibition of protein synthesis (Korsnes et al., 2014) and which the ribosomes are main targets for ribotoxic stress.

The pathways of normal ribosome turnover are not well known. However, ribosome recycling through association with the endoplamic reticulum. Accumulation in vacuolar structures have been observed in yeast and Arabidopsis RNS2 suggesting a ribophagy-like mechanism targeting ribosomes (MacIntosh and Bassham, 2011). Normal rRNA decay is therefore necessary to maintain cellular homeostasis. Autophagic activity induced by YTX through ribophagy may in this case be essential for rRNA recycling.

Lamellar bodies may evolve from cytoplasmic lipid droplets involving membranes of ER and Golgi (Schmitz and Müller, 1991). Cells exposed to YTX contain various lamellar bodies associated with lipid droplets (Figs. 2, 3 and 4).

Formation of lamellar bodies have been associated with defective lipid transport, defect in normal processing of lipoproteins or autophagic activities of the cells (Schmitz and Müller, 1991). The presence of numerous lamellar bodies under YTX exposure suggest alteration in the lipid metabolism. The specific degradation of lipid droplets represents a type of selective autophagy called lipophagy (Klionsky et al., 2012) and which might take place in the present treated cells.

The analysis of LC3 fluorescent puncta serve to monitor the autophagy flux. Fluorescence microscopy reveals that YTX exposure tends to increase LC3 punctae over time suggesting increased numbers of autophagosomes after start of exposure (Figs. 5, 6 and 7). Starvation treatment for 18 h in control and YTX-treated cells evidenced induction of autophagy. Combined treatment of bafilomycin A1 and YTX increased the amount of the LC3-II cytoplasmatic puncta. A possible explanation might be that YTX acts as an autophagic inducer blocking autophagic flux in downstream steps of the autophagic pathway (Fig. 8).

Western blotting analyses in YTX-treated cells reveal conversion from endogenous LC3-I to LC3-II. An advantage in measuring autophagic flux based on the ratio between LC3-I and LC3-II, is that it does not require the presence of autophagic inhibitors to block degradation of LC3-II (Klionsky et al., 2012). The amount of LC3-II usually correlates well with autophagosomes, although LC3-II can also be generated in autophagy-independent manner and it has been detected in lipid droplets (Shibata et al., 2009; Mizushima et al., 2010). Additional assays are therefore needed to monitor autophagy.

Measurements of SQSTM1/p62 expression can demonstrate increased autophagic flux (Bjørkøy et al., 2006). This protein accumulates in completed autophagosomes and degrade in autolysosomes. Decreased levels of it indicate increase in levels of autophagy. The present Western blotting analysis reveals such decrease in YTX-exposed cells (Fig. 14). Downregulation of p62 was significant at 24 h and 48 h, however at 72 h was less significant. Accumulation of protein aggregates due to cellular stress can upregulate p62 indicating defective autophagy (Bjørkøy et al., 2006).

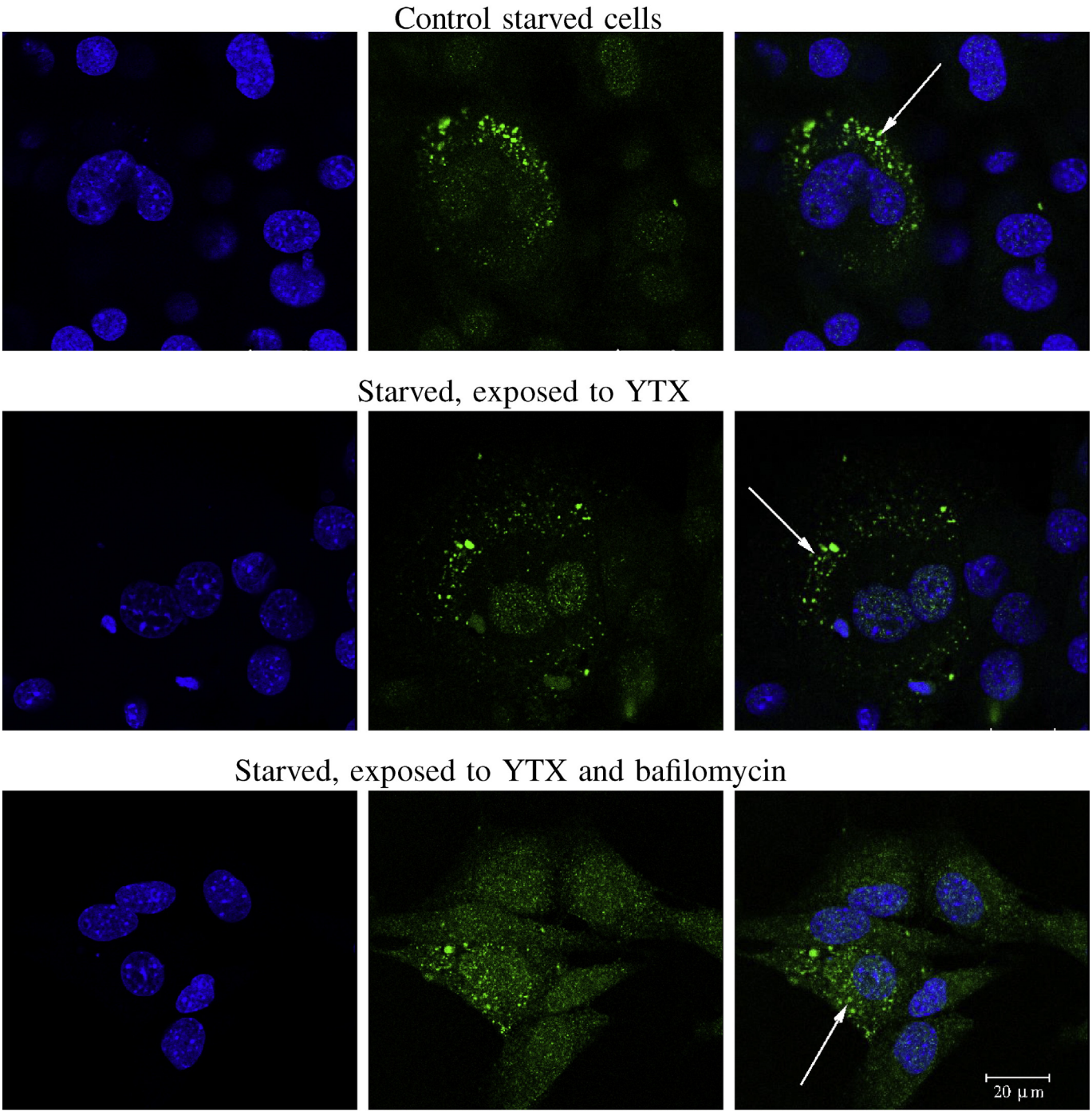

Fig. 8. Immunofluorescence detection of cytoplasmatic LC3-II puncta in BC3H1 cells subjected to starvation treatment for 18 h. Upper row: Starved untreated BC3H1 cells. Left: Hoechst labelling showing nuclei. Middle: Starved untreated BC3H1 cells. Right: Two-colour overlay with Hoechst and FITC showing cytoplasmic puncta. Middle row: Starved cells exposed to 100 nM YTX. Left: Hoechst labelling showing nuclei. Middle: Starved BC3H1 cells exposed to 100 nM YTX. Right: Two-colour overlay with Hoechst and FITC showing cytoplasmic puncta. Lower row: YTX-treated cells with 10 nM bafilomycin. Left: Hoechst labelling showing nuclei. Middle: BC3H1 cells exposed for 24 h with 100 nM YTX and 10 nM bafilomycin. Right: Immunofluorescence staining of endogeneous LC3-II visualised as a cytoplasmatic puncta representing autophagosomes. Arrows show punctuate pattern indicating the formation of autophagosomes. The results are representative for more than three independent experiments.

Research on yeast revealed the function of Atg proteins in autophagosome formation (Klionsky et al., 2003). Such formation involves Atg-conjugation systems (Mizushima et al., 2011). Atg16 is for yeast required for pre-autophagosomal formation where it facilitates co-localization of At12 and Atg5 proteins to form the Atg12–Atg5–Atg16 complex. This complex contributes to stabilise incipient phagohores (Madeo et al., 2015). Atg16 is therefore associated with formation of the phagophore, but not with completed autophagosomes upon induction of autophagy (Ravikumar et al., 2010). Levels of Atg16 increase with time in the YTX-treated cells, suggesting an active generation of double-membrane vesicles to ingest cytoplasmic material.

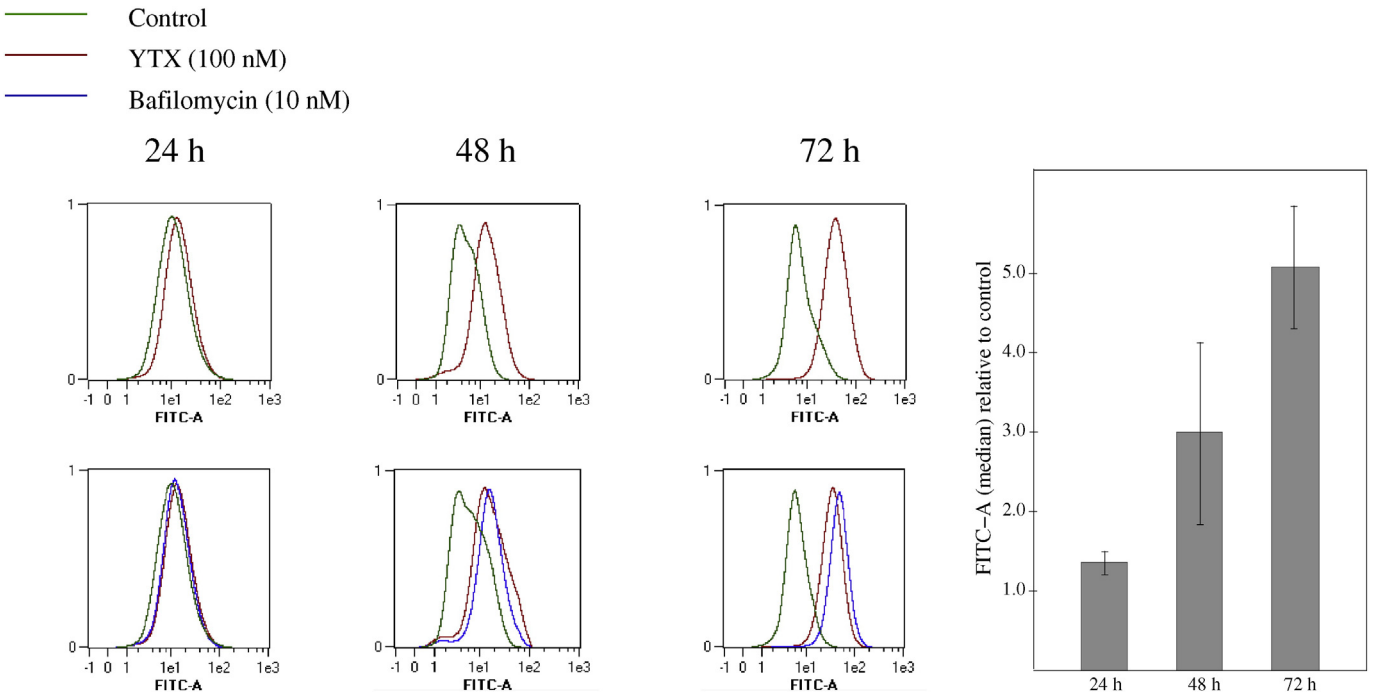

Fig. 9. Autophagic flux determination of LC3-II using flow-cytometry. BC3H1 cells treated with 100 nM YTX and 10 nM bafilomycin during 24 h, 48 h, and 72 h. Treatment with YTX shows an increase in green fluorescence compared to control. Bafilomycin-treated cells in the presence of 100 nM YTX show a slight increase in the fluorescence signal only at 24 h. Right: median values of FITC-A for YTX-treated cells from 3 independent experiments (95% confidence intervals).

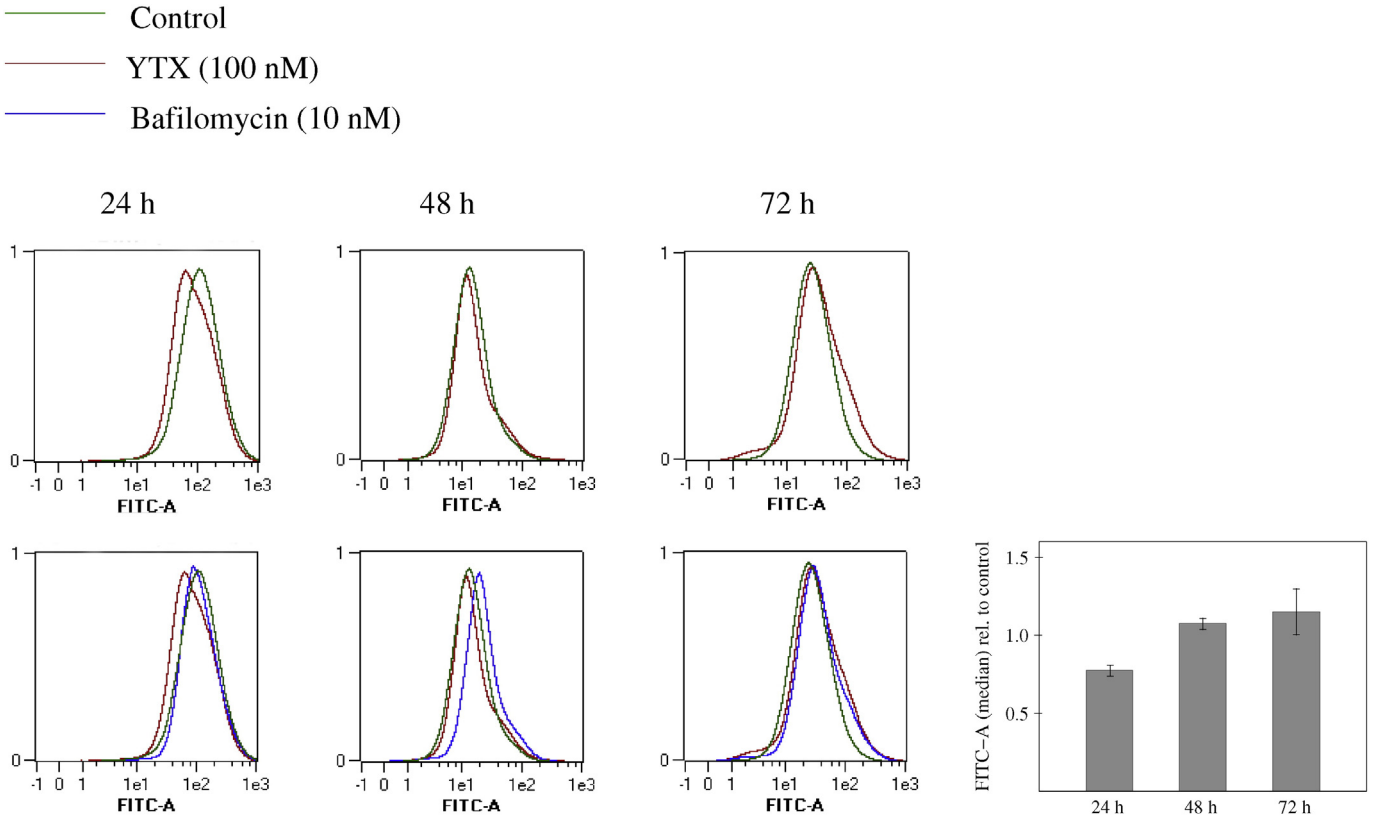

Fig. 10. Autophagic flux determination of SQSTM1/p62 using flow-cytometry. BC3H1 cells treated with 100 nM YTX and 10 nM bafilomycin during 24 h, 48 h, and 72 h. Treatment with YTX shows a decrease in green fluorescence compared to control. Bafilomycin-treated cells in the presence of 100 nM YTX show similarly as LC3-II a slight increase in the fluorescence signal only at 24 h. The results are representative of at least three independent experiments. Right: median values of FITC-A for YTX-treated cells from 3 independent experiments (95% confidence intervals).

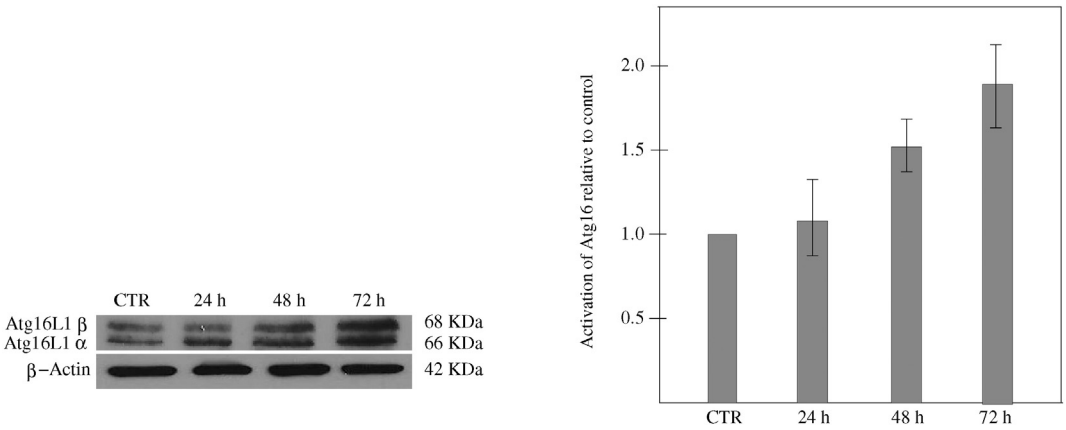

Fig. 11. Western blot analysis showing Atg16 activation in BC3H1 cells treated with 100 nM YTX for 24, 48 and 72 h. Left: Representative Western blot analysis showing activation of Atg16. Actin was used as a loading control. Right: Expression levels, relative to control, from 3 independent experiments (95% confidence intervals).

Increased autophagic activity can explain the observed upregulation of Beclin-1 in YTX-treated cells. Upregulation of Beclin has been observed during autophagic cell death (Tsujimoto and Shimizu, 2005). However, cell death appears to be at least partly independent of autophagy, since YTX can induce different cell death pathways in BC3H1 cells (Korsnes, 2012; Korsnes and Korsnes, 2015). Beclin is assumed to be the only Atg-protein specific for autophagy, since embryonic lethality is observed in mice deficient for Beclin-1 (Qu et al., 2003; Yue et al., 2003). Beclin-1 can also be detected upon apoptosis induction and its binding to Bcl-2 or Bcl-xL has been suggested in the cross-talk between autophagy and apoptotic cell death (Pattingre et al., 2005; Maiuri et al., 2007; Scott et al., 2007; Wirawan et al., 2010). Lethal activation of caspases or calpains, however, can result in digestion of Beclin-1, hence inactivating the autophagic machinery (Yousefi et al., 2006; Djavaheri-Mergny et al., 2010).

The present flow-cytometry analysis to determine autophagic flux (Fig. 9) allows detection of endogenous LC3-II in single cells in a population. This additional analysis may therefore strengthen the meaning of the data since it assesses a combination of morphology and immunofluorescence patterns providing statistically meaningful data (Yang and Klionsky, 2010b). The fluorescence signal from single cells appeared to increase with time. This result differs from Western blotting analysis at 72 h (Fig. 13). These differences may arise from the sensitivity of the methods to asses conjugation of the LC3-II to the autophagosomal membrane. Flow-cytometry analysis provides signals from single (complete) cells within a population accumulating LC3-II up to 72 h. Western blotting analysis, on the contrary, provides a measure of LC3-II concentration in lysed cells including fractions of cells dying before 72 h. The variability in individual cell fate can therefore be masked in aggregate properties. Single cell analyses over time may promote awareness of this diversity (Korsnes and Korsnes, 2015).

Bafilomycin A1 treatment was partially able to inhibit LC3-II turnover during the first 24 h of YTX exposure (Fig. 9). Such treatment had no apparent effect on p62 (Fig. 10). A possible interpretation of these results would be that bafilomycin A1, especially at the concentration of 10 nM, does not prevent YTX-induced death by altering autophagosome formation and/or recycling. Bafilomycin A1 either induces autophagy as a survival response to YTX or attenuates the YTX-induced inhibition of autophagy. However, bafilomycin A1 treatment can vary significantly within the same cell lines and with

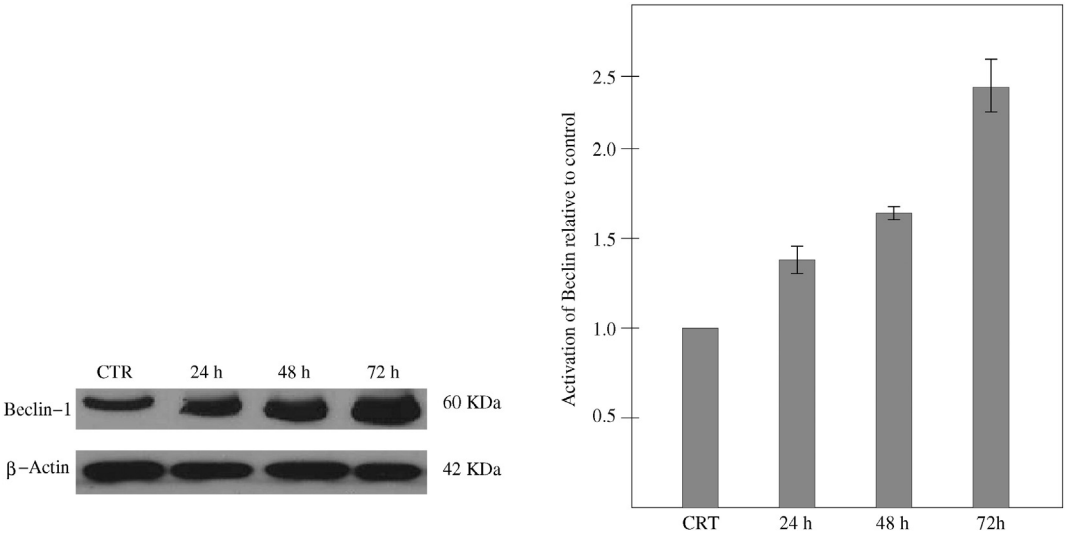

Fig. 12. Western blot analysis showing temporal increase of Beclin activation in BC3H1 cells treated with 100 nM YTX for 24, 48 and 72 h. Left: Representative Western blot analysis showing Beclin activation. Actin was used as a loading control. Right: Expression levels, relative to control, from 3 independent experiments (95% confidence intervals).

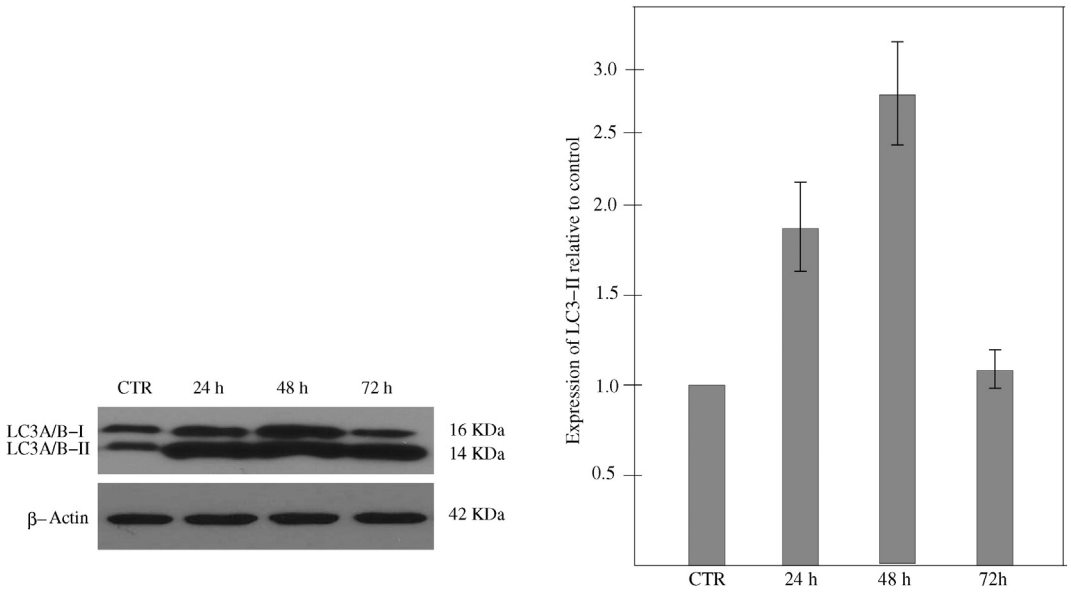

Fig. 13. Western blot analysis showing LC3-II ratio in BC3H1 cells treated with 100 nM YTX for 24, 48 and 72 h. Left: Representative Western blot analysis showing LC3-II expression. Actin was used as a loading control. Right: Expression levels, relative to control, from 3 independent experiments (95% confidence intervals). Increased levels of LC3-II were reached up to 72 h, where the maximum observed level was at 48 h.

similar concentrations (Klionsky et al., 2008). Duration of the treatment also influences its effect making it difficult to give a correct interpretation of the results.

Inhibition of autophagy correlates with increased levels of p62 in mammals and Drosophila whereas activation of autophagy correlates with decreased levels of p62 (Cui et al., 2012). Flow-cytometry shows downregulation of p62 for BC3H1 cells exposed to YTX for 24 h suggesting autophagic activity (Fig. 10). Western blotting analyses of LC3-II and p62 similarly indicate increased autophagosome formation and induction of autophagy.

Eukaryotic cells synthesise proteins on soluble ribosomes or on ribosomes attached to the ER (Yorimitsu et al., 2006). Each reaction in the ribosome assembly pathway, particularly within translation, is monitored since rRNA sequences that have been the most highly conserved throughout evolution, are probably prime targets for monitoring by surveillance (Lafontaine, 2010). Defective translation of proteins by damaged ribosomes might allow accumulation of potential harmful proteins allowing ribotoxic stress to take place. Clearance of defective ribosomes may therefore be critical to preserve cellular homeostasis.

Ribotoxic stress can potentially trigger autophagic activity in cells exposed to YTX. Stress responses can generally dispatch danger signals known as "damaged associated molecular patterns" (DAMPs). They operate upon binding to receptors expressed by bystander cells, including cellular components of both the innate and adaptive immune system. They require the establishment of a pre-mortem ER stress response and induction of autophagy where autophagic responses are required for dying cells to secrete ATP (Bezu et al., 2015).

YTX triggers a robust ER stress response leading to autophagic cell death in glioma cells (Rubiolo et al., 2014). DAMPS emission in response to stress responses including ER and ribotoxic stress in dying cells exposed YTX exposure might therefore be plausible. YTX could accordingly trigger immunogenic cell death (ICD) depending on emission of DAMPS under stress conditions and which is a non-conventional type of apoptosis. This type of cell death is associated with activation of an adaptive immune response against dead cell-associated antigens (Kroemer et al., 2013). It depends on components of the apoptotic apparatus (Galluzzi et al., 2012) and YTX has shown to be an efficient apoptotic inducer (Korsnes and Espenes, 2011). However, this possibility needs to be investigated since it can add further complexity to this small molecular compound as a novel immunogenic cell death inducer with the capability to stimulate anticancer immuno responses.

There seems to be a potential cross-talk between ribotoxic stress-induced autophagy and cell death pathways. This work also indicates a link or signalling pathway between ribotoxic stress and autophagy. However, the mechanism by which ribosomes are selected as autophagic cargo is unknown. Such knowledge can help better to

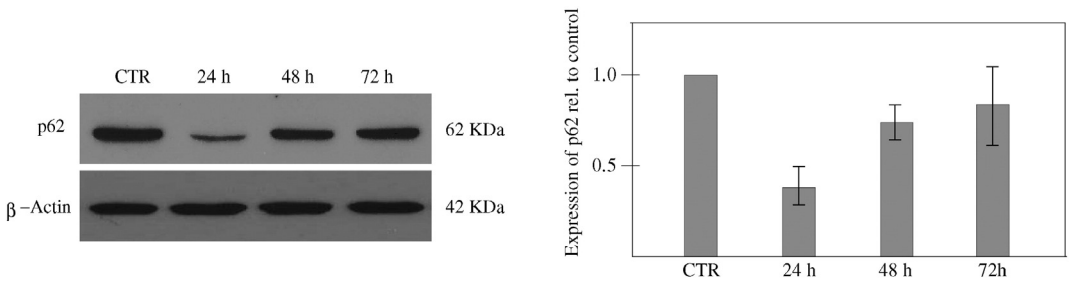

Fig. 14. Western blot analysis showing expression levels of p62 in BC3H1 cells treated with 100 nM YTX for 24, 48 and 72 h. Left: Representative Western blot analysis showing p62 downregulation. Actin was used as a loading control. Right: Expression levels, relative to control, from 3 independent experiments (95% confidence intervals).

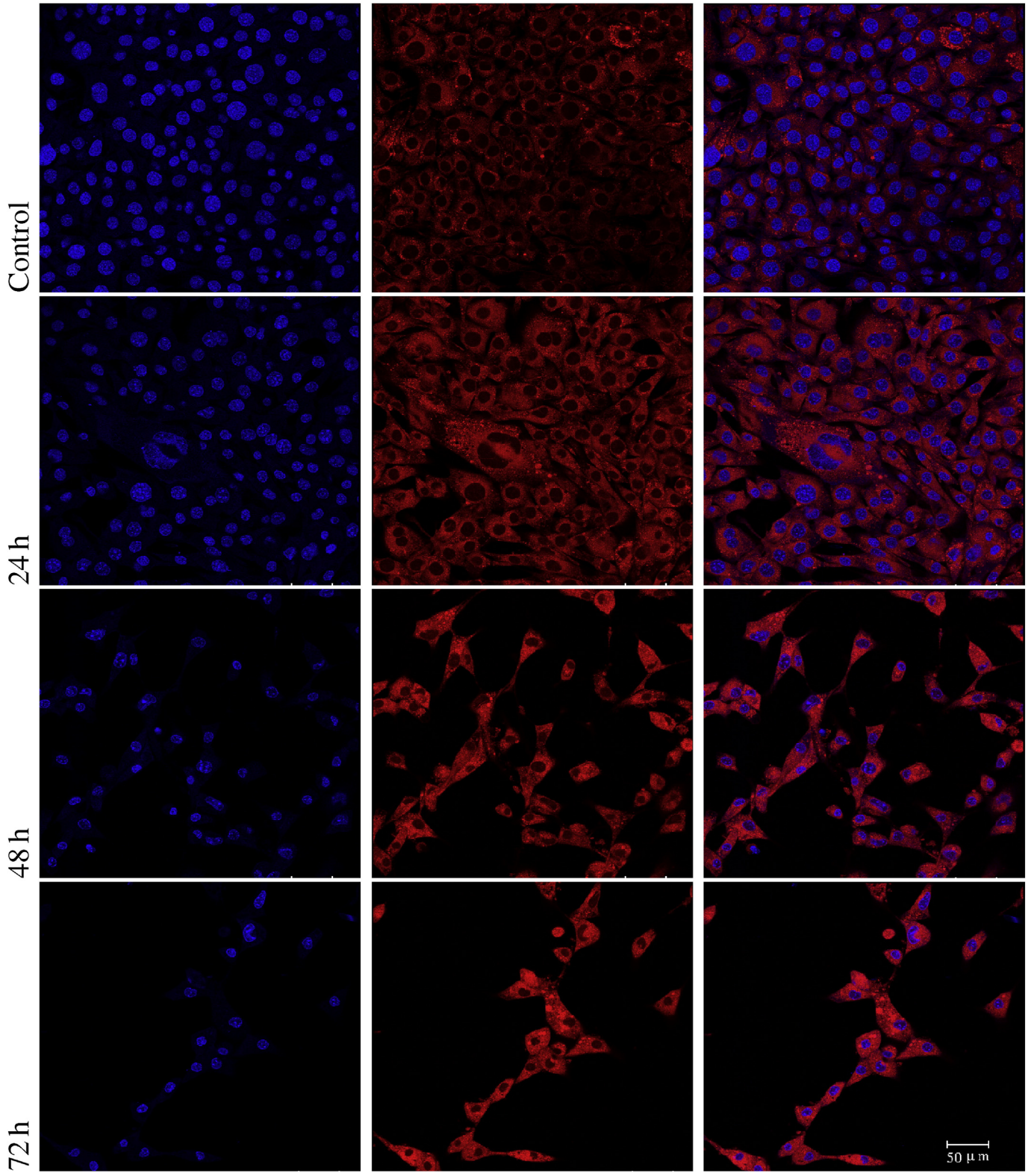

Fig. 15. Immunofluorescence detection of acidic vacuoles in BC3H1 cells exposed to 100 nM YTX using LysoTracker Red DND-99 Staining. Upper row: Control cells. Left: Hoechst labelling showing nuclei. Middle: Untreated BC3H1 cells labelled with LysoTracker Red. Right: Two-colour overlay with Hoechst and LysoTracker. Note scarce acidic compartments (red puncta). Second, third and lower row: Cells exposed to 100 nM YTX for 24 h, 48 h, and 72 h respectively. Left: Hoechst labelling showing nuclei. Middle: BC3H1 cells exposed to 100 nM YTX. Right: Two-colour overlay with Hoechst and LysoTracker Red showing acidic vacuoles (red puncta). Note that the amount of acidic vacuoles increases upon YTX-treatment. The results are representative for more than two independent experiments.

understand how autophagy in diseases associates with ribotoxic stress. Further research might clarify links between ribotoxic stress and autophagy and indentify ways for pharmacological exploitation of YTX to induce signalling pathways that can serve as potential targets for cancer therapy or to stimulate anticancer immune responses.

Transparency document

The Transparency document associated with this article can be found in the online version.

Acknowledgements

This study was supported by Olav Raagholt og Gerd Meidel Raagholts Legacy, Astri og Birger Torsteds Legacy and Giske og Peter Jacob Sørensen Research Foundation.

References

Alfonso, A., de la Rosa, L., Vieytes, M.R., Yasumoto, T., Botana, L.M., 2003. Yessotoxin, a novel phycotoxin, activates phosphodiesterase activity: effect of yessotoxin on cAMP levels in human lymphocytes. Biochem. Pharmacol. 65, 193–208.
Alonso, E., Vale, C., Vieytes, M.R., Botana, L.M., 2013. Translocation of PKC by yessotoxin in an in vitro model of Alzheimer disease with improvement of tau and β-amyloid pathology. ACS Chem. Neurosci. 4, 1062–1070.
Bezu, L., Gomes-de Silva, L.C., Dewitte, H., Breckpot, K., Fucikova, J., Spisek, R., Galluzzi, L., Kepp, O., Kroemer, G., 2015. Combinatorial strategies for the induction of immunogenic cell death. Front. Immunol. 6.
Biazik, J., Ylä-Anttila, P., Vihinen, H., Jokitalo, E., Eskelinen, E.L., 2015. Ultrastructural relationship of the phagophore with surrounding organelles. Autophagy 11, 439–451.
Bjørkøy, G., Lamark, T., Johansen, T., 2006. p62/SQSTM1: a missing link between protein aggregates and the autophagy machinery. Autophagy 2, 138–139.
Callegari, F., Rossini, G.P., 2008. Yessotoxin inhibits the complete degradation of E-cadherin. Toxicology 244, 133–144.
Cui, D., Wang, L., Qi, A., Zhou, Q., Zhang, X., Jiang, W., 2012. Propofol prevents autophagic cell death following oxygen and glucose deprivation in PC12 cells and cerebral ischemia–reperfusion injury in rats. PLoS One 7, e35324.
De la Rosa, L., Alfonso, A., Vilarino, N., Vieytes, M.R., Yasumoto, T., Botana, L.M., 2001. Modulation of cytosolic calcium levels if human lymphocytes by yessotoxin, a novel marine phycotoxin. Biochem. Pharmacol. 61, 827–833.
Djavaheri-Mergny, M., Maiuri, M., Kroemer, G., 2010. Cross talk between apoptosis and autophagy by caspase-mediated cleavage of Beclin 1. Oncogene 29, 1717–1719.
Draisci, R., Ferretti, E., Palleschi, L., Marchiafava, C., Poletti, R., Milandri, A., Ceredi, A., Pompei, M., 1999. High levels of yessotoxin in mussels and presence of yessotoxin and homoyessotoxin in dinoflagellates of the Adriatic Sea. Toxicon 37, 1187–1193.
Eskelinen, E.L., 2008. To be or not to be? Examples of incorrect identification of autophagic compartments in conventional transmission electron microscopy of mammalian cells. Autophagy 4, 257–260.
Eskelinen, E.L., Reggiori, F., Baba, M., Kovács, A.L., Seglen, P.O., 2011. Seeing is believing: the impact of electron microscopy on autophagy research. Autophagy 7, 935–956.
Fernández-Araujo, A., Alfonso, A., Vieytes, M., Botana, L., 2015. Key role of phosphodiesterase 4A (PDE4A) in autophagy triggered by yessotoxin. Toxicology 329.
Franchini, A., Marchesini, E., Poletti, R., Ottaviani, E., 2004. Lethal and sub-lethal yessotoxin dose-induced morpho-functional alterations in intraperitoneal injected Swiss CD1 mice. Toxicon 44, 83–90.
Galluzzi, L., Vitale, I., Abrams, J.M., Alnemri, E.S., Baehrecke, E.H., Blagosklonny, M.V., Dawson, T.M., Dawson, V.L., El-Deiry, W.S., Fulda, S., et al., 2012. Molecular definitions of cell death subroutines: recommendations of the Nomenclature Committee on Cell Death 2012. Cell Death Differ. 1, 107–120.
Hamasaki, M., Furuta, N., Matsuda, A., Nezu, A., Yamamoto, A., Fujita, N., Oomori, H., Noda, T., Haraguchi, T., Hiraoka, Y., et al., 2013. Autophagosomes form at ER-mitochondria contact sites. Nature 495, 389–393.
Klionsky, D., Cregg, J., Dunn, W., Emr, S., Sakai, Y., Sandoval, N., Sibirny, A., Subramani, S., Thumm, M., Veenhuis, M., Ohsumi, Y., Klionsky, D., Cregg, J., Dunn, J., Emr, S., Sandoval, I., 2003. A unified nomenclature for yeast autophagy-related genes. Dev. Cell 5, 539–545.
Klionsky, D.J., Abeliovich, H., Agostinis, P., Agrawal, D.K., Aliev, G., Askew, D.S., Baba, M., Baehrecke, E.H., Bahr, B.A., Ballabio, A., Bamber, B.A., Bassham, D.C., Bergamini, E., Bi, X., Biard-Piechaczyk, M., Blum, J.S., Bredesen, D.E., Brodsky, J.L., Brumell, J.H., Brunk, U.T., Bursch, W., Camougrand, N., Cebollero, E., Cecconi, F., Chen, Y., Chin, L.S., Choi, A., Chu, C.T., Chung, J., Clarke, P.G., Clark, R.S., Clarke, S.G., Clave, C., Cleveland, J.L., Codogno, P., Colombo, M.I., Coto-Montes, A., Cregg, J.M., Cuervo, A.M., Debnath, J., Demarchi, F., Dennis, P.B., Dennis, P.A., Deretic, V., Devenish, R.J., Sano, F.D., Dice, J.F., Difiglia, M., Dinesh-Kumar, S., Distelhorst, C.W., Djavaheri-Mergny, M., Dorsey, F.C., Droge, W., Dron, M., Dunn, J., Duszenko, M., Eissa, N.T., Elazar, Z., Esclatine, A., Eskelinen, E.L., Fesus, L., Finley, K.D., Fuentes, J.M., Fueyo, J., Fujisaki, K., Galliot, B., Gao, F.B., Gewirtz, D.A., Gibson, S.B., Gohla, A., Goldberg, A.L., Gonzalez, R., Gonzalez-Estevez, C., Gorski, S., Gottlieb, R.A., Haussinger, D., He, Y.W., Heidenreich, K., Hill, J.A., Hoyer-Hansen, M., Hu, X., Huang, W.P., Iwasaki, A., Jaattela, M., Jackson, W.T., Jiang, X., Jin, S., Johansen, T., Jung, J.U., Kadowaki, M., Kang, C., Kelekar, A., Kessel, D.H., Kiel, J.A., Kim, H.P., Kimchi, A., Kinsella, T.J., Kiselyov, K., Kitamoto, K., Knecht, E., et al., 2008. Guidelines for the use and interpretation of assays for monitoring autophagy in higher eukaryotes. Autophagy 4, 151–175.
Klionsky, D.J., Abdalla, F.C., Abeliovich, H., Abraham, R.T., Acevedo-Arozena, A., Adeli, K., Agholme, L., Agnello, M., Agostinis, P., Aguirre-Ghiso, J.A., et al., 2012. Guidelines for the use and interpretation of assays for monitoring autophagy. Autophagy 8, 445–544.
Korsnes, M.S., 2012. Yessotoxin as a tool to study induction of multiple cell death pathways. Toxins 4, 568–579.
Korsnes, M.S., Espenes, A., 2011. Yessotoxin as an apoptotic inducer. Toxicon 57, 947–958.
Korsnes, M.S., Korsnes, R., 2015. Lifetime distributions from tracking individual BC3H1 cells subjected to yessotoxin. Front. Bioeng. Biotechnol. 3.
Korsnes, M.S., Hetland, D.L., Espenes, A., Tranulis, M.A., Aune, T., 2006. Apoptotic events induced by yessotoxin in myoblast cell lines from rat and mouse. Toxicol. in Vitro 20, 1077–1087.
Korsnes, M.S., Espenes, A., Hetland, D.L., Hermansen, L.C., 2011. Paraptosis-like cell death induced by yessotoxin. Toxicol. in Vitro 25, 1764–1770.
Korsnes, M.S., Espenes, A., Hermansen, L.C., Loader, J.I., Miles, C.O., 2013. Cytotoxic responses in BC3H1 myoblast cell lines exposed to 1-desulfoyessotoxin. Toxicol. in Vitro 27, 1962–1969.
Korsnes, M.S., Røed, S.S., Tranulis, M.A., Espenes, A., Christophersen, B., 2014. Yessotoxin triggers ribotoxic stress. Toxicol. in Vitro 28, 975–981.
Kroemer, G., Galluzzi, L., Brenner, C., 2007. Mitochondrial membrane permeabilization in cell death. Physiol. Rev. 87, 99–163.
Kroemer, G., Mariño, G., Levine, B., 2010. Autophagy and the integrated stress response. Mol. Cell 40, 280–293.
Kroemer, G., Galluzzi, L., Kepp, O., Zitvogel, L., 2013. Immunogenic cell death in cancer therapy. Annu. Rev. Immunol. 31, 51–72.
Lafontaine, D.L., 2010. A 'garbage can' for ribosomes: how eukaryotes degrade their ribosomes. Trends Biochem. Sci. 35, 267–277.
Levine, B., 2005. Eating oneself and uninvited guests: autophagy-related pathways in cellular defense. Cell 120, 159–162.
Levine, B., Kroemer, G., 2008. Autophagy in the pathogenesis of disease. Cell 132, 27–42.
Levine, B., Kroemer, G., 2009. Autophagy in aging, disease and death: the true identity of a cell death impostor. Cell Death Differ. 16, 1–2.
Liang, X.H., Jackson, S., Seaman, M., Brown, K., Kempkes, B., Hibshoosh, H., Levine, B., 1999. Induction of autophagy and inhibition of tumorigenesis by beclin 1. Nature 402, 672–676.
López, L.M.B., Rancano, A.A., Vieytes, M.R., Garcia, M.I.L., 2008. Therapeutic use of yessotoxins as human tumor cell growth inhibitors, EPO Patent EP1875906.
López, A.M., Rodrguez, J.J.G., Mirón, A.S., Camacho, F.G., Grima, E.M., 2011a. Immunoregulatory potential of marine algal toxins yessotoxin and okadaic acid in mouse T lymphocyte cell line EL-4. Toxicol. Lett. 207, 167–172.
López, L.M.B., López, E.A., Gonzalez, C.V., 2011b. Use of yessotoxin and analogues and derivatives thereof for treating and/or preserving neurodegenerative diseases linked to tau and beta amyloid, European Patent Application PCT/ES2011/070078.
Ma, Y., Galluzzi, L., Zitvogel, L., Kroemer, G., 2013. Autophagy and cellular immune responses. Immunity 39, 211–227.
MacIntosh, G.C., Bassham, D.C., 2011. The connection between ribophagy, autophagy and ribosomal RNA decay. Autophagy 7, 662–663.
Madeo, F., Zimmermann, A., Maiuri, M.C., Kroemer, G., 2015. Essential role for autophagy in life span extension. J. Clin. Invest. 125, 85.
Maiuri, M.C., Le Toumelin, G., Criollo, A., Rain, J.C., Gautier, F., Juin, P., Tasdemir, E., Pierron, G., Troulinaki, K., Tavernarakis, N., et al., 2007. Functional and physical interaction between Bcl-XL and a BH3-like domain in Beclin-1. EMBO J. 26, 2527–2539.
Malagoli, D., Marchesini, E., Ottaviani, E., 2006. Lysosomes as the target of yessotoxin in invertebrate and vertebrate cell lines. Toxicol. Lett. 167, 75–83.
Martn-López, A., Gallardo-Rodrguez, J.J., Sánchez-Mirón, A., Garca-Camacho, F., Molina-Grima, E., 2012. Cytotoxicity of yessotoxin and okadaic acid in mouse T lymphocyte cell line EL-4. Toxicon 60, 1049–1056.
Mizushima, N., Levine, B., Cuervo, A.M., Klionsky, D.J., 2008. Autophagy fights disease through cellular self-digestion. Nature 451, 1069–1075.
Mizushima, N., Yoshimori, T., Levine, B., 2010. Methods in mammalian autophagy research. Cell 140, 313–326.
Mizushima, N., Yoshimori, T., Ohsumi, Y., 2011. The role of Atg proteins in autophagosome formation. Annu. Rev. Cell Dev. Biol. 27, 107–132.
Murata, M., Kumagai, M., Lee, J.S., Yasumuto, T., 1987. Isolation and structure of yessotoxin, a novel polyether compound implicated in diarrhetic shellfish poisining. Tetrahedron Lett. 28, 5869–5872.
Orhon, I., Dupont, N., Pampliega, O., Cuervo, A., Codogno, P., 2014. Autophagy and regulation of cilia function and assembly. Cell Death Differ. 1–9.
Orsi, C.F., Colombari, B., Callegari, F., Todaro, A.M., Ardizzoni, A., Rossini, G.P., Blasi, E., Peppoloni, S., 2010. Yessotoxin inhibits phagocytic activity of macrophages. Toxicon 55, 265–273.
Pattingre, S., Tassa, A., Qu, X., Garuti, R., Liang, X.H., Mizushima, N., Packer, M., Schneider, M.D., Levine, B., 2005. Bcl-2 antiapoptotic proteins inhibit Beclin 1-dependent autophagy. Cell 122, 927–939.
Pattingre, S., Bauvy, C., Carpentier, S., Levade, T., Levine, B., Codogno, P., 2009. Role of JNK1-dependent Bcl-2 phosphorylation in ceramide-induced macroautophagy. J. Biol. Chem. 284, 2719–2728.
Qu, X., Yu, J., Bhagat, G., Furuya, N., Hibshoosh, H., Troxel, A., Rosen, J., Eskelinen, E.L., Mizushima, N., Ohsumi, Y., et al., 2003. Promotion of tumorigenesis by heterozygous disruption of the beclin 1 autophagy gene. J. Clin. Invest. 112, 1809.
Ravikumar, B., Moreau, K., Jahreiss, L., Puri, C., Rubinsztein, D.C., 2010. Plasma membrane contributes to the formation of pre-autophagosomal structures. Nat. Cell Biol. 12, 747–757.
Ronzitti, G., Rossini, G.P., 2008. Yessotoxin induces the accumulation of altered E-cadherin dimers that are not part of adhesive structures in intact cells. Toxicology 244, 145–156.
Rubiolo, J., López-Alonso, H., Martnez, P., Millán, A., Cagide, E., Vieytes, M., Vega, F., Botana, L., 2014. Yessotoxin induces ER-stress followed by autophagic cell death in glioma cells mediated by mTOR and BNIP3. Cell. Signal. 26, 419–432.

Satake, M., MacKenzie, L., Yasumoto, T., 1997. Identification of *Protoceratium reticulatum* as the biogenetic origin of yessotoxin. Nat. Toxins 4, 164–167.
Satake, M., Ichimura, T., Sekiguchi, K., Yoshimatu, S., Oshima, Y., 1999. Confirmation of yessotoxin and 45,46,47-trinoryessotoxin production by *Protoceratium reticulatum* collected in Japan. Nat. Toxins 7, 147–150.
Schmitz, G., Müller, G., 1991. Structure and function of lamellar bodies, lipid–protein complexes involved in storage and secretion of cellular lipids. J. Lipid Res. 32, 1539–1570.
Scott, R.C., Juhász, G., Neufeld, T.P., 2007. Direct induction of autophagy by Atg1 inhibits cell growth and induces apoptotic cell death. Curr. Biol. 17, 1–11.
Shibata, M., Yoshimura, K., Furuya, N., Koike, M., Ueno, T., Komatsu, M., Arai, H., Tanaka, K., Kominami, E., Uchiyama, Y., 2009. The MAP1-LC3 conjugation system is involved in lipid droplet formation. Biochem. Biophys. Res. Commun. 382, 419–423.
Shimizu, S., Kanaseki, T., Mizushima, N., Mizuta, T., Arakawa-Kobayashi, S., Thompson, C.B., Tsujimoto, Y., 2004. Role of Bcl-2 family proteins in a non-apoptotic programmed cell death dependent on autophagy genes. Nat. Cell Biol. 6, 1221–1228.
Tallóczy, Z., Virgin IV, H., Levine, B., 2006. PKR-dependent xenophagic degradation of herpes simplex virus type 1. Autophagy 2, 24–29.
Tsujimoto, Y., Shimizu, S., 2005. Another way to die: autophagic programmed cell death. Cell Death Differ. 12, 1528–1534.
Wirawan, E., Walle, L.V., Kersse, K., Cornelis, S., Claerhout, S., Vanoverberghe, I., Roelandt, R., De Rycke, R., Verspurten, J., Declercq, W., et al., 2010. Caspase-mediated cleavage of Beclin-1 inactivates Beclin-1-induced autophagy and enhances apoptosis by promoting the release of proapoptotic factors from mitochondria. Cell Death Dis. 1, e18.
Yang, Z., Klionsky, D.J., 2010a. Eaten alive: a history of macroautophagy. Nat. Cell Biol. 12, 814–822.
Yang, Z., Klionsky, D.J., 2010b. Mammalian autophagy: core molecular machinery and signaling regulation. Curr. Opin. Cell Biol. 22, 124–131.
Yorimitsu, T., Nair, U., Yang, Z., Klionsky, D.J., 2006. Endoplasmic reticulum stress triggers autophagy. J. Biol. Chem. 281, 30299–30304.
Young, C., Truman, P., Boucher, M., Keyzers, R., Northcote, P., Jordan, W.T., 2009. The algal metabolite yessotoxin affects heterogeneous nuclear ribonucleoproteins in HepG2 cells. Proteomics 9, 2529–2542.
Yousefi, S., Perozzo, R., Schmid, I., Ziemiecki, A., Schaffner, T., Scapozza, L., Brunner, T., Simon, H.U., 2006. Calpain-mediated cleavage of Atg5 switches autophagy to apoptosis. Nat. Cell Biol. 8, 1124–1132.
Yu, L., Alva, A., Su, H., Dutt, P., Freundt, E., Welsh, S., Baehrecke, E.H., Lenardo, M.J., 2004. Regulation of an ATG7-beclin 1 program of autophagic cell death by caspase-8. Science 304, 1500–1502.
Yue, Z., Jin, S., Yang, C., Levine, A.J., Heintz, N., 2003. Beclin 1, an autophagy gene essential for early embryonic development, is a haploinsufficient tumor suppressor. Proc. Natl. Acad. Sci. U. S. A. 100, 15077–15082.